Effect of acyl chain unsaturation on the packing of model diacylglycerols in simulated monolayers

Kenneth R. Applegate and John A. Glomset

Regional Primate Research Center, Departments of Biochemistry and Medicine, and Howard Hughes Medical Institute Laboratories, SL-15, University of Washington, Seattle, WA 98195

Abstract In a companion study of the effects of acyl chain unsaturation on a series of model *sn*-1,2-diacylglycerols (DGs) we showed that individual DGs could adopt one of three energy-minimized conformations depending on the number and location of *cis* double bonds in the *sn*-2 chain. Here we show that each of these conformations promotes a distinct type of packing arrangement in a simulated DG monolayer. One conformation, shown by *sn*-1-18:0 DGs containing an *sn*-2 22:6(n-3)-, 20:4(n-6)-, or 20:3(n-9)- group, determines a regular packing that resembles a known hybrid subcell, HS2, of crystalline hydrocarbon chains. The second conformation, shown by DGs containing an *sn*-2 18:0-, 18:2(n-6)-, or 18:3(n-3)- group, determines a regular packing that resembles a second known, distinct hydrocarbon subcell, HS1. The third conformation, that of 18:0/18:1(n-9) DG, determines a much looser, less energetically favorable packing. Stable heterogeneous packings are possible for DGs that have similar conformations, but mixed packings of DGs that have dissimilar conformations are less stable. These results raise the possibility that differences in *sn*-2 acyl chain unsaturation among membrane *sn*-1,2-diacylglycerophospholipids may promote the formation of different domains. —**Applegate, K. R., and J. A. Glomset.** Effect of acyl chain unsaturation on the packing of model diacylglycerols in simulated monolayers. *J. Lipid Res.* 1991. **32:** 1645-1655.

Supplementary key words docosahexaenoic acid • arachidonic acid • eicosatrienoic acid • stearic acid • linoleic acid • linolenic acid • oleic acid

We have been using a computer-based molecular modeling approach to investigate aspects of the structure of polyenoic fatty acids that might influence intermolecular interactions among phospholipids in animal cell membranes (1). In a companion study of a series of *sn*-1-18:0 DGs containing different *sn*-2 fatty acyl groups having 0 to 6 double bonds (2), we showed that the energy-minimized conformations of these DGs could be classified into three types based on the number and location of *cis* double bonds in the *sn*-2 fatty acyl chain. DGs with *sn*-2 fatty acyl chains that contained angle-iron-shaped polyenoic segments (1) could adopt one of two essentially straight conformations, which showed different contacts between the *sn*-1 and *sn*-2 chains, depending on the location of the first double bond in the polyenoic sequence. In contrast, 18:0/18:1 (n-9) DG adopted a third type of conformation that was irregular. We show below that each of the three different conformations identified for individual DGs determines a distinct packing arrangement in a simulated monolayer.

METHODS

Computer resources

We used the integrated biomedical package, PROPHET (3, 4), as described previously (1, 2). In addition, an extension of the MOLXSECTION program calculated the volumes occupied by packed DGs as the sum of products of area times slice thickness for a set of uniform cross-sectional projections. We wrote two new programs to help us determine initial positions for DGs in a packed array. The first program moved a DG relative to one or more fixed DGs (all having orientations specified by the user) so that it occupied successive positions on a specified rectangular grid. The initial MMP2 steric energy was computed at each grid point without further energy minimization. The Prophet public procedure CONTOUR (5) then produced plots of steric energy versus relative position that were used to locate minimum energy packing configurations. The second, interactive program allowed the user to reorient and move one or more DGs in a packed array along predetermined paths while displaying a space-filling view of the configuration and providing tal-

Abbreviations: DG, diacylglycerol; 12:0/12:0 DG, *sn*-1,2-dilauroylglycerol; 16:0/16:0 DG, *sn*-1,2-dipalmitoyl diacylglycerol; 18:0/18:0 DG, *sn*-1,2-distearoylglycerol; 18:0/18:1(n-9) DG, *sn*-1-stearoyl-2-oleoylglycerol; 18:0/18:2(n-6) DG, *sn*-1-stearoyl-2-linoleoylglycerol; 18:0/18:3(n-3) DG, *sn*-1-stearoyl-2-linolenoylglycerol; 18:0/20:3(n-9) DG, *sn*-1-stearoyl-2-(5,8,11)-eicosatrienoylglycerol; 18:0/20:4(n-6) DG, *sn*-1-stearoyl-2-arachidonoylglycerol; 18:0/ 22:6(n-3) DG, *sn*-1-stearoyl-2-docosahexaenoylglycerol; PE, phosphatidylethanolamine; 12:0/12:0 PE, *sn*-1,2-dilauroyl phosphatidylethanolamine; PC, phosphatidylcholine; PA, phosphatidic acid; HS1, hybrid subcell 1; HS2, hybrid subcell 2.

lies of the number of van der Waals contacts and overlaps for each position.

Homogeneous packings of DGs

We modeled the close packing of DGs in planar, hexagonal arrays, the smallest repeating units that could be tiled by simple translations to yield a complete monolayer. Such arrays sampled all of the nearest neighbor interactions experienced by a central DG. Each DG, optimized previously (2), was oriented with its acyl chain axes normal to the model monolayer. We used the *sn*-2 ester oxygen atom (O21), which was situated approximately between the two chain axes, as an arbitrary internal coordinate origin for each DG and a center for positioning it in the hexagonal cell. Then we used MM2 to optimize the intra- and intermolecular interactions.

Refinement of the packing models within the maximum atom limitations for MMP2 (500 atoms) required extraction of adjoining triplet or quartet arrays from the hexagonal cells and their separate optimization. The MMP2 results could then be combined, with corrections for edge effects, to estimate packing energies and areas per DG molecule for the complete hexagonal cells and for hexagonally packed infinite monolayers. Specific methods for assembling hexagonal cells containing various DGs are described below.

18:0/22:6(n-3) DG, 18:0/20:4(n-6) DG, and 18:0/20:3(n-9) DG. To find packing geometries mutually compatible with acyl chain and oxygen dipole interactions among 18:0/22:6(n-3) DGs in a monolayer, we first constructed full contour maps of steric energy versus position and orientation on a 1 Å grid for two and three truncated 10:0/14:4(n-0) DGs (used to reduce computation time). The minimum energy "valleys" indicated the proper location and orientation for positioning full length 18:0/22:6(n-3) DGs in a hexagonal array which was then optimized using MMP2.

For 18:0/20:4(n-6) DG or 18:0/20:3(n-9) DGs we created an initial hexagonal array with the DGs occupying the same positions and orientations as observed for the refined packing of 18:0/22:6(n-3) DGs. We then used limited contour mapping of interaction energy (18:0/20:4(n-6) DG packing) or interactive adjustment of van der Waals contact distances (18:0/20:3(n-9) DG packing) to produce modified hexagonal arrays for further MMP2 refinement.

18:0/18:0 DG, 18:0/18:2(n-6) DG, or 18:0/18:3(n-3) DG. We used a three-step approach to model the packing of 18:0/18:0 DGs. We first created a hexagonal array of DL-12:0/12:0 DGs, using mirror images of a model minimized previously (2). The packing model had unit cell dimensions, molecule positions, and orientations corresponding to those obtained from Cambridge Crystal File data for crystalline DL-12:0/12:0 PE (6, 7). Next we generated a packing model for D-12:0/12:0 DG. We converted L isomers in the DL packing model of 12:0/12:0 DG to D isomers by reflecting the L isomers through planes that were normal to the monolayer and passed through the axes of both hydrocarbon chains. Limited energy contour mapping was used to adjust the model and reduce overlap of some ester oxygens. Finally, we generated a model of packed D- isomers of 18:0/18:0 DG having the same lattice positions and orientations, and optimized the model using MMP2.

We created two different hexagonal arrays of 18:0/18:2(n-6) DG, corresponding to the optimized packing models for 18:0/18:0 DGs and 18:0/20:4(n-6) DGs, respectively. We then interactively adjusted the positions of 18:0/18:2(n-6) DGs in each model to optimize van der Waals contacts before refining the models using MMP2. Since the conformation of the 18:0/18:3(n-3) DG was similar to that of the 18:0/18:2(n-6) DG (2), we placed it in the positions and orientations found for the first (lower energy) optimized packing of 18:0/18:2(n-6) DGs described above, and adjusted positions by the same method before refining the model using MMP2.

18:0/18:1(n-9) DGs could not be positioned and oriented well on the hexagonal lattices found for the other DGs. We searched for possible packings of 18:0/18:1(n-9) DGs by extensive interactive examination of van der Waals contacts for many relative positions and orientations normal to the monolayer. The configurations producing the best fit were incorporated in a hexagonal array and refined using MMP2. We did not examine tilted orientations of the DGs because these would have produced unreasonably large apparent molecular areas.

Heterogeneous packings of DGs

We created the following mixed packings: *a*) 18:0/22:6(n-3) DG + 18:0/20:4(n-6) DG; *b*) 18:0/20:4(n-6) DG + 18:0/18:2(n-6) DG; and *c*) 18:0/18:0 DG + 18:0/18:2(n-6) DG. The first two models were based upon the 18:0/22:6(n-3) DG homogeneous packing, while the third was based on the 18:0/18:0 DG packing. To include all possible nearest-neighbor interactions in a spatially uniform 1:1 mixture, we modeled two arrays, each centered on a different DG component. Each array consisted of a central row of DGs of one type, bracketed by rows of the other. We adjusted positions and orientations of DGs in each array by the methods described, and then abstracted all unique triplet configurations for refinement by MMP2. The results were recombined in the correct ways to represent each of the distinct hexagonal arrays. Then the results for the two optimized arrays were combined to obtain the average geometry and energies for the 1:1 mixed monolayer.

Analysis of refined models

Packing geometry. We averaged any small difference in the separation of DGs in overlapping triplets or quartets, and

used the averaged distances between O21 atoms to regenerate the hexagonal cell. We determined parameters of cell geometry from atom coordinates in the array, and determined the area of the hexagon by simple geometry using the O21 positions as vertices. We computed cross-sectional areas for projections and slices of the models parallel to the monolayer plane with the MOLXSECTION program (1).

Volumes occupied by the packed DGs were computed using the extension of the MOLXSECTION program described earlier. We defined the volume of the packing cell to lie within the projected hexagon, between a proximal bounding plane through the O21 atoms, and a distal plane through the final carbon of the shorter *sn*-2 chain. The latter choice excluded spurious void volume which would be filled in a real lipid membrane by interdigitation with the opposite leaflet. The void volume contained within the hexagonal cell was the difference between the total geometric cell volume and the volume occupied by the DGs within its boundaries.

Packing energy. We defined this as the difference between the MMP2 steric energies for packed arrays and those for all isolated component DGs. The calculation was done most easily by combining the packing energies for pairwise interactions of DGs. MMP2 initial energy computations on subsets of individual DGs and DG pairs from the minimized arrays yielded the intermolecular part of the pairwise packing energies. Differences in steric energy between isolated, minimized DG conformations and the conformations after minimization in the packed array determined intramolecular packing energies resulting from internal conformational changes.

We corrected for edge effects in triplet arrays by formally assuming that each array contained one-half of each pairwise interaction and one-sixth of each component DG (for a total of one-half DG per triplet). Thus, the intermolecular packing energy per DG for each triplet was the sum of the three pairwise packing energies, and the intramolecular packing energy was one-third the sum of the intramolecular packing energies for the components. We estimated packing energies for the hexagonal cells or larger patches of monolayer by summing corrected packing energies of component triplets.

RESULTS

Packings of 18:0/22:6(n-3)-, 18:0/20:4(n-6)-, and 18:0/20:3(n-9) DGs (Type 1 DGs)

Our previous study (1) of hexaenoic hydrocarbon chains containing a sequence of methylene-interrupted *cis* double bonds similar to that found in 22:6(n-3) showed that such chains packed effectively in a back-to-back, antiparallel arrangement. In addition, we had identified optimal packings of the hexaenoic hydrocarbon chains with saturated chains. It was therefore of interest to determine whether the packing of 18:0/22:6(n-3) DGs and other Type 1 DGs would be governed by similar types of molecular interactions. A systematic study of optimum relative orientations and positions (Methods) revealed highly ordered packing geometries (**Fig. 1** and **Fig. 2**). As shown in Fig. 1 for 18:0/22:6(n-3) DG, similarly oriented DGs were aligned in parallel (horizontal) rows, which alternated with rows of DGs having an antiparallel orientation. The polyenoic *sn*-2 chains in the adjacent rows of DGs were stacked together in a back-to-back antiparallel arrangement that was very similar to that described previously for single hexaenoic hydrocarbons (1). One angle-iron plane of each DG packed in a location that was almost identical to that found for the hydrocarbons, while the other, located on the side of the DG having a projecting *sn*-2 carbonyl group, required a somewhat greater separation and offset. The stacking of the angle-irons had several effects: *1*) it led to the above-mentioned antiparallel orientation of the DGs in adjacent rows; *2*) it caused an offset of about half a molecule for adjacent rows; *3*) it allowed each *sn*-1 chain, already rotated to fit the *sn*-2 angle-iron within a DG (2), to come simultaneously into close contact with an adjoining *sn*-2 angle-iron in the same row and with *sn*-1 chains in adjacent rows of DGs in configurations similar to those found for hydrocarbon chains (1); *4*) it permitted optimum antiparallel intermolecular dipole interactions between pairs of carbonyl groups in the rotated *sn*-1 chains; and *5*) it permitted antiparallel dipole interactions between pairs of *sn*-2 carbonyl groups positioned correctly by the half-molecule offsets and antiparallel orientation of DGs in adjacent rows.

The optimized hexagonal packing cells for all the Type 1 DGs had similar overall dimensions, although differences of 0.2–0.4 Å in the positions of corresponding DGs in the three cells produced some differences in cell shape and internal parameters such as row separations and offsets (**Table 1**). The molecular cross-sectional areas

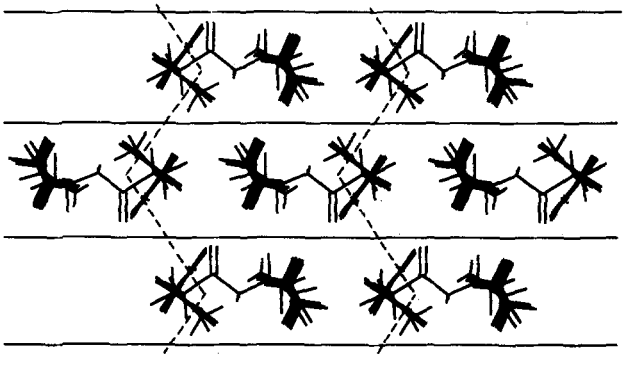

Fig. 1. Detailed geometry of 18:0/22:6(n-3) DG packing cell. The DGs are shown in full Dreiding projection of all atoms and bonds onto the cell plane. Solid lines separate the antiparallel rows of DGs, while dotted lines trace the pleated sheets of interacting angle-iron configurations of polyenoic chains transverse to the rows.

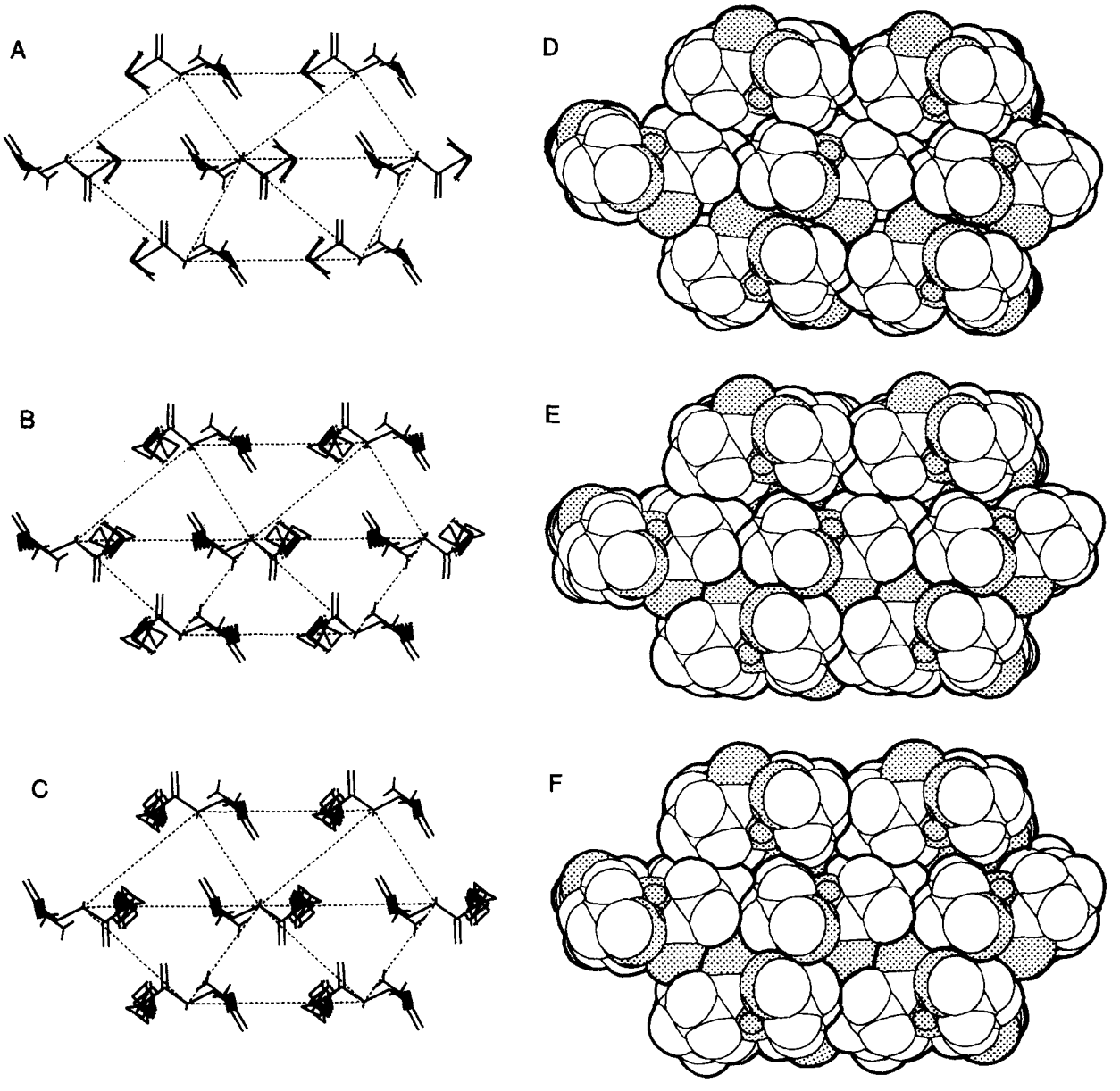

Fig. 2. Comparative geometry of hexagonal packing cells for Type 1 DGs. Packed DGs are shown in Dreiding projection of backbone carbon and oxygen atoms and bonds onto the cell plane (parts A-C). Cell outlines between O21 atoms are shown by dotted lines. DGs are also shown in space-filling projections, as viewed from the polar end of each molecule (parts D-F). Oxygen atoms are emphasized by light gray stippling. Heavy lines indicate molecular boundaries. DGs are: (A,D), 18:0/22:6(n-3) DG; (B,E), 18:0/20:4(n-6) DG; (C,F), 18:0/20:3(n-9) DG.

for all three DGs were only a few percent larger than that calculated for crystalline 12:0/12:0 PE (8), and the internal void volumes were all negligible (**Table 2**). There was a slight increase (2.5%) in the cross-sectional area/DG in going from the packing of 18:0/22:6(n-3) DG, with its very regular angle-iron-shaped chains, through 18:0/20:4(n-6) DG to 18:0/20:3(n-9) DG with increasing lengths of saturated segments in the *sn*-2 chains. However, the increased area/DG had no significant effect on the calculated packing densities. Similar packing energies indicative of strong intermolecular interactions and tight packing were obtained for all three DGs (**Table 3**). The somewhat greater packing energy for 18:0/20:3(n-9) DG relative to the two other DGs may reflect an increased contribution to van der Waals interactions from the larger number of saturated segments in its *sn*-2 chains.

Because Type 1 DGs pack similarly, in an arrangement henceforward referred to as a Type 1 packing, favorable heterogeneous packings of the DGs might be expected. To test this possibility we studied the packing of a 1:1 mixture of 18:0/22:6(n-3) DGs and 18:0/20:4(n-6) DGs (Methods). The optimized packing showed a hexagonal cell geometry

TABLE 1. Geometric data for hexagonal packing cells of DGs, measured in the plane of a simulated monolayer

DG Packing Model	Packing Type	Cell Half Length	Cell Height	Row 1 Height	Row 2 Height	Row 1,2 Offset	Row 1,2 Offset Angle	Row 1,3 Offset	Row 1,3 Offset Angle	Row 1 Mol Rotation	Row 2 Mol Rotation
18:0/18:0	Type 2	7.71	10.51	5.97	4.54	4.08	55.69	0.15	89.19	- 33.91	- 153.05
18:0/18:1(n-9)	Type 3	7.74	12.14	7.60	4.55	2.05	74.88	- 0.97	94.56	- 34.16	142.62
18:0/18:2(n-6)	Type 2	7.86	10.17	5.83	4.35	2.94	63.20	- 0.03	90.18	- 34.03	- 144.03
18:0/18:2(n-6)	Type 1	10.00	9.51	5.36	4.15	2.76	62.76	- 0.02	90.11	- 0.93	179.07
18:0/18:3(n-3)	Type 2	7.86	10.17	5.72	4.45	3.00	62.28	- 0.03	90.18	- 35.48	- 145.47
18:0/20:3(n-9)	Type 1	8.80	9.48	4.82	4.66	3.64	52.97	0.65	86.10	1.48	- 178.52
18:0/20:4(n-6)	Type 1	8.80	9.48	4.70	4.78	3.58	52.73	0.65	86.10	1.83	- 178.17
18:0/22:6(n-3)	Type 1	8.87	9.33	5.04	4.28	2.89	60.15	- 0.18	91.10	- 0.73	179.27

DGs are listed by acyl chain composition and type of packing. Distances are given in Ångstroms, and angles in degrees counterclockwise from the horizontal base of the cell. DG locations are determined by the positions of O21 atoms in the bridge between acyl chains. The horizontal separation between DGs in the projected array is the cell half-length, while the cell height measures the separation between alternate rows of DGs. Row 1,2 and row 2,3 heights are separations of individual rows. Row 1,2 and row 1,3 offsets and offset angles measure the horizontal translation and angular skew of adjacent and alternate rows of DGs. DG rotations refer to a line passing through the two points defined by the projected mean positions of carbon atoms in the portions of the *sn*-1 and *sn*-2 chains normal to the monolayer.

that was intermediate between those of the corresponding homogeneous packings (Table 1). The packing energy was 3% and 6% smaller, respectively, than those of the corresponding homogeneous packings (Table 3), possibly because of the mirror image geometry of the angle-iron-shaped segments in the two types of DG. As a result of this geometry, double bonds in adjacent DGs of the mixed packing were staggered at different levels and may not have interacted optimally.

Packings of 18:0/18:0-, 18:0/18:2(n-6)-, and 18:0/18:3(n-3) DGs (Type 2 DGs)

Because the optimum molecular conformation previously found for 18:0/18:0 DG (2) was very similar to that of the diacylglyceryl moiety of 12:0/12:0 PE, we created a packing model for 18:0/18:0 DG that was derived from the known structure of crystalline DL-12:0/12:0 PE (7, 9). We found that some expansion of the crystallographic cell was necessary to accommodate an array of D-isomers, as opposed to the racemic crystals used in the X-ray studies (Methods). However, the general shape of the hexagonal packing cell and the orientation of molecules in it were similar to those in the crystal structure (**Fig. 3**). 18:0/18:0 DGs having an oblique orientation were arranged in alternate parallel rows, while 18:0/18:0 DGs of the intervening rows had a different oblique orientation. As a result, the DGs formed a zigzag pattern transverse to the row direction, which interlocked the molecules of adjacent rows. This packing geometry arose because of the Type 2 DG conformation in which proximal, saturated segments of the two acyl chains lie in mutually parallel, but offset planes, with exact, vertical interdigitation of methylene hydrogen atoms (2). The tight interlocking and orientation of the chains made it necessary to rotate the entire DG to allow the acyl chains of different rows to come into close intermolecular contact. Then, closely packed clusters of three chains from three different DG molecules appeared to stabilize the network by interdigitation of methylene groups. In the intervening regions, the chains interacted by non-interdigitating van der Waals contacts

TABLE 2. Projected cross-sectional areas and volumes for separate DGs and DGs packed in hexagonal arrays

DG	Packing Type	DG Area/ Molecule	Packing Cell Area/ Molecule	Percent Area Reduction	DG Volume/ Molecule	Packed Volume/ Molecule	Percent Volume Reduction	Percent Empty Volume
18:0/18:0	Type 2	50.41	40.50	19.69	907.4	797.5	12.1	6.9
18:0/18:1(n-9)	Type 3	62.43	46.87	25.71	914.4	802.2	12.2	11.6
18:0/18:2(n-6)	Type 2	53.41	39.98	25.16	878.0	781.4	11.0	1.3
18:0/18:2(n-6)	Type 1	53.41	47.52	11.58	878.0	853.5	2.8	9.3
18:0/18:3(n-3)	Type 2	55.71	40.23	27.78	887.6	717.3	19.2	1.2
18:0/20:3(n-9)	Type 1	54.94	42.70	22.28	960.7	867.2	9.7	1.0
18:0/20:4(n-6)	Type 1	55.65	41.73	24.95	903.2	821.6	9.0	0.2
18:0/22:6(n-3)	Type 1	52.42	41.36	21.14	953.0	859.0	9.9	1.2

DGs are listed by acyl chain composition and type of packing. Areas/molecule are in $Å^2$, while volumes/molecule are in $Å^3$. Cross-sectional areas were determined for the projection of the entire DG or packed array on the monolayer plane, with standard MMP2 van der Waals radii for atoms. Percent area reduction refers to the decrease in apparent area as an isolated DG is placed in a packed array. Approximate volumes were computed from projected areas for slices of uniform cross-section parallel to the monolayer. The percent empty (void) volume was determined from the difference between total cell volume and volume occupied by DGs within the cell (see Methods).

TABLE 3. Packing energies for hexagonal arrays of DGs

Packings of DGs	Packing Domain	Packing Energy		
		Intramol.	Intermol.	Total
Homogeneous				
18:0/18:0	Type 2	0.08	− 48.45	− 48.37
18:0/18:1(n-9)	Type 3	− 0.18	− 31.80	− 31.99
18:0/18:2(n-6)	Type 2	0.08	− 51.20	− 51.12
18:0/18:2(n-6)	Type 1	− 0.22	− 36.88	− 37.10
18:0/18:3(n-3)	Type 2	1.11	− 52.08	− 50.97
18:0/20:3(n-9)	Type 1	0.60	− 53.81	− 53.21
18:0/20:4(n-6)	Type 1	− 0.02	− 50.45	− 50.47
18:0/22:6(n-3)	Type 1	0.33	− 51.71	− 51.37
Heterogeneous				
3 18:0/22:6(n-3)* + **4** 18:0/20:4(n-6)	Type 1	1.28	− 49.63	− 48.35
4 18:0/22:6(n-3) + **3** 18:0/20:4(n-6)*	Type 1	1.20	− 49.95	− 48.74
Avg 1:1 mixture		1.24	− 49.79	− 48.55
3 18:0/18:2(n-6)* + **4** 18:0/20:4(n-6)	Type 1	− 0.08	− 40.40	− 40.48
4 18:0/18:2(n-6) + **3** 18:0/20:4(n-6)*	Type 1	− 0.18	− 40.70	− 40.87
Avg 1:1 mixture		− 0.13	− 40.55	− 40.68
3 18:0/18:0* + **4** 18:0/18:2(n-6)	Type 2	0.89	− 44.53	− 43.64
4 18:0/18:0 + **3** 18:0/18:2(n-6)*	Type 2	0.38	− 50.57	− 50.18
Avg 1:1 mixture		0.64	− 47.55	− 46.91

Energies are in kcal/mole. Corrections were made for edge effects, so that the values apply to monolayers of any size. For homogeneous packings, a single hexagonal cell modeled all unique interactions. For heterogeneous packings, two complementary hexagonal cells were required, each with a central row of one species of DG, bracketed by rows of the second species of DG. The central DG in each cell is indicated by an asterisk, and each DG is prefixed by its relative amount in the cell. Energies are given separately for each type of cell, followed by the average energy for both cells, which represents a true 1:1 molar ratio.

at greater chain separations, but those regions contained clusters of three ester carbonyl groups that were arranged so their dipoles interacted to produce a mutual attraction.

Because the optimized Type 2 molecular conformations found for 18:0/18:2(n-6) DG and 18:0/18:3(n-3) DG were very similar to that found for 18:0/18:0 DG (2), we examined the possibility that those DGs would pack in a common packing mode. We found that they did indeed pack in similar hexagonal arrays, henceforth referred to as a Type 2 packing (**Fig. 4**). The overall dimensions of the arrays were similar (Table 1), and the rotational angles of the oriented DGs were similar as well. However, the spacing of the DGs differed somewhat, as also noted for the Type 1 packings. The average cross-sectional areas/DG were all very close to the value of 40 $Å^2$ (Table 2), often found experimentally for phospholipids having two saturated chains and small head groups (8). Even though the isolated 18:0/18:3(n-3) DG model had a large cross-sectional area, it packed as well as the other two Type 2 DGs. Packing densities for the 18:0/18:2(n-6) DGs and 18:0/18:3(n-3) DGs were as high as for Type 1 DGs, with negligible void volumes. However, the void volume in the 18:0/18:0 DG packing was 7% because the small cross-sectional area of tightly interdigitated saturated chains was smaller than the cross-sectional area of the glyceryl ester region.

The net effect of these interactions was to produce a stabilizing effect. The packing energy for Type 2 DGs was of similar magnitude to that found for Type 1 packings (Table 3). The packing energies for 18:0/18:2(n-6) DGs and 18:0/18:3(n-3) DGs were actually larger than that for 18:0/18:0 DGs, due to the less dense packing of the latter. It is noteworthy that fitting the rather large cross-section of 18:0/18:3(n-3) DG into a tight Type 2 packing was accomplished at the expense of about 1 kcal/mole of intramolecular packing energy for internal rearrangement of its conformation.

We also tested whether 18:0/18:2(n-6) DGs could pack in the Type 1 geometry, but obtained a much poorer fit (**Fig. 5**). The long dimension in the packing required expansion (Table 1) to accommodate the intramolecular spacing and axial orientation of the *sn*-1 and *sn*-2 chains

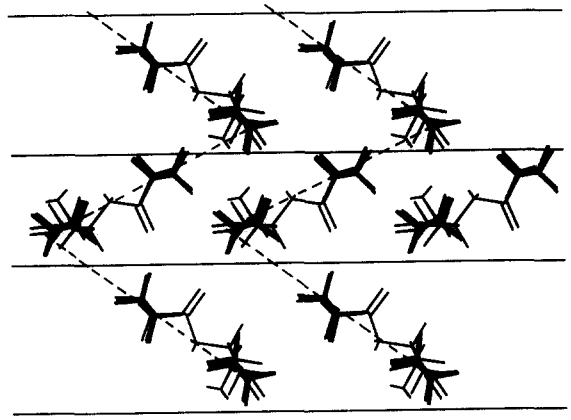

Fig. 3. Detailed geometry of 18:0/18:0 DG packing cell. The DG molecules are shown in full Dreiding projection as in Fig. 1. Solid lines separate the rows of rotated DGs.

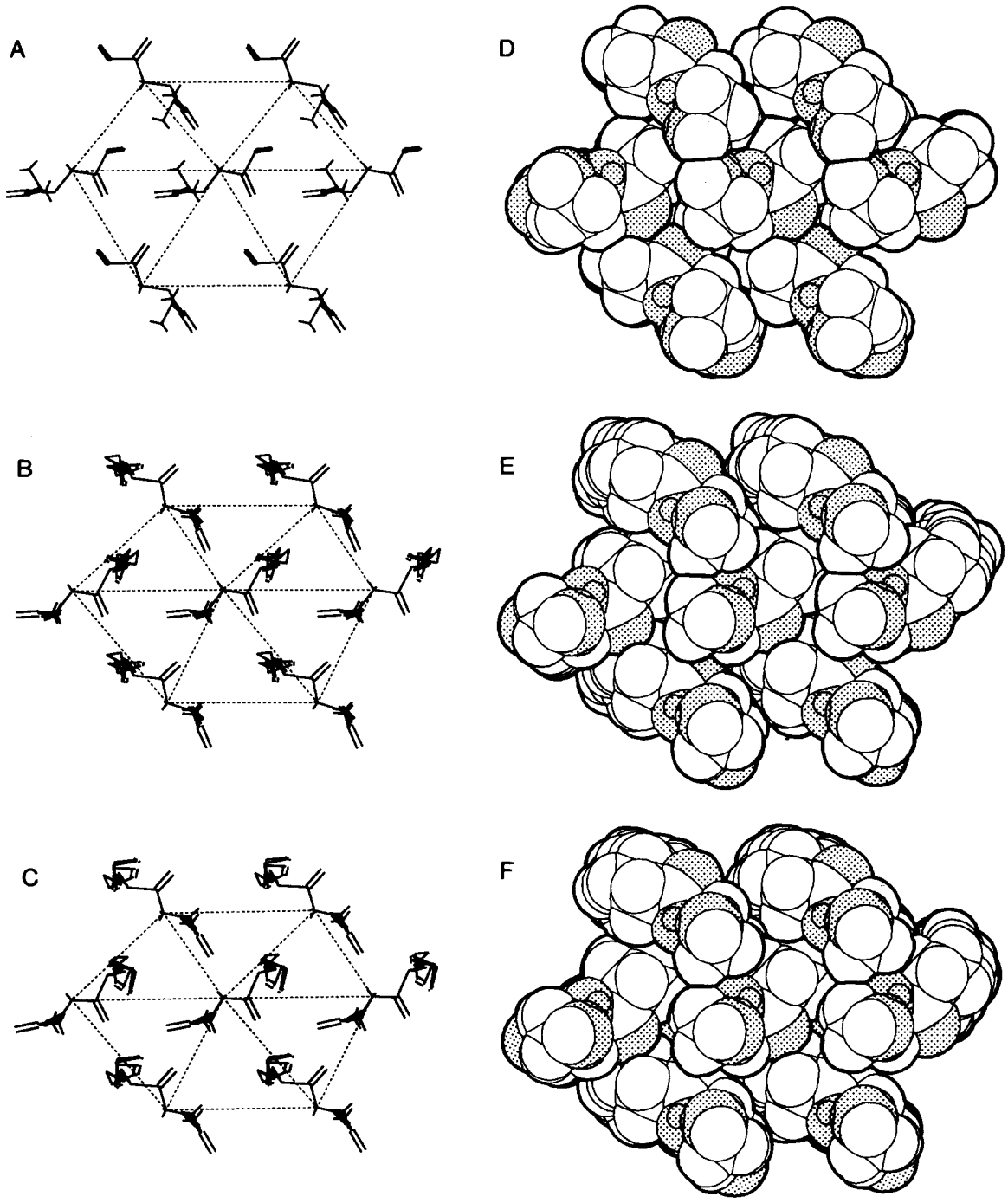

Fig. 4. Comparative geometry of hexagonal packing cells for Type 2 DGs. Packed DG molecules are shown in Dreiding and space-filling projections as in Fig. 2. DGs are: (A,D), 18:0/18:0 DG; (B,E), 18:0/18:2(n-6) DG; (C,F), 18:0/18:3(n-3) DG.

(compare Fig. 4B with 5B). Therefore, the internal void volume of the Type 1 packing was 9.3% as compared with 1.3% for the alternative packing (Table 2). Furthermore, intermolecular contacts were weaker, and the packing energy was about 25% smaller than that of the Type 2 packing (Table 3). Thus, the Type 1 packing of 18:0/18:2(n-6) DGs was poor even though the back-to-back packings of angle-iron segments that stabilized other Type 1 packings were present. (Such back-to-back packings were absent in the stable Type 2 packing of this DG.)

Although pure 18:0/18:2(n-6) DGs did not pack well in a Type 1 array, we wanted to see whether the presence of a Type 1 DG could promote a better packing. Therefore, we paired 18:0/18:2(n-6) DGs with 18:0/20:4(n-6) DGs in

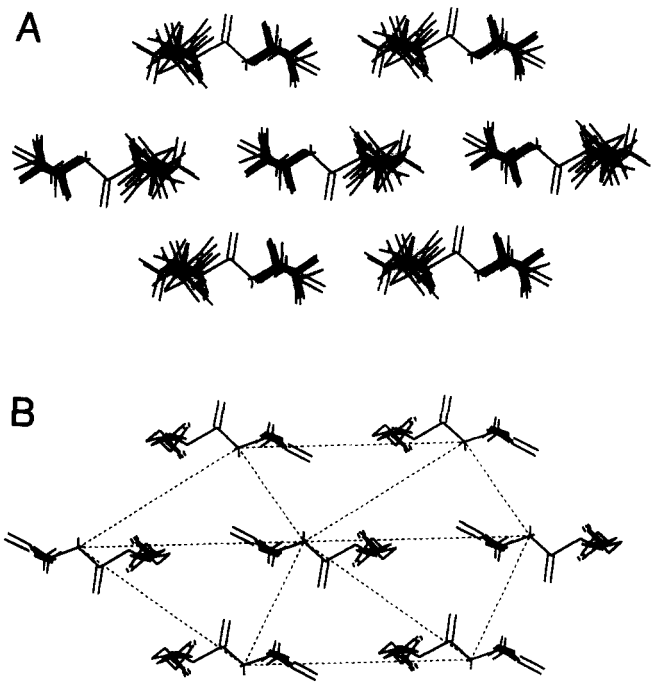

Fig. 5. Geometry of Type 2 18:0/18:2(n-6) DG in a Type 1 packing cell. A) The DG molecules are shown in full Dreiding projection of all atoms and bonds onto the cell plane. Note the elongation of the packing cell and lower packing density compared with Fig. 1 or Fig. 3. B) DG molecules are shown in Dreiding projection of backbone carbon and oxygen atoms and bonds onto the cell plane. Cell outlines between O21 atoms are shown by dotted lines.

a 1:1 ratio in a Type 1 packing array. The mutual fit of 18:0/18:2(n-6) DGs and 18:0/20:4(n-6) DGs in the Type 1 packing was poor compared to the fit of 18:0/18:2(n-6) DGs and 18:0/18:0 DGs in the Type 2 packing. Furthermore, the packing energy was 20% smaller than that found for the homogeneous packing of 18:0/20:4(n-6) DGs (Table 3). Nevertheless, the mixed Type 1 packing of 18:0/18:2(n-6) DGs and 18:0/20:4(n-6) DGs was less distorted than the corresponding Type 1 packing of pure 18:0/18:2(n-6) DGs.

To determine whether a 1:1 mixture of Type 2 DGs would pack favorably, we studied the packing of 18:0/18:0 DGs with 18:0/18:2(n-6) DGs. We found that this packing required little modification of the molecular positions or orientations found for the respective homogeneous packings. The packing energy, averaged over 18:0/18:0 DG- and 18:0/18:2(n-6) DG-centered arrays (Methods), was 8.5% smaller than that found for the homogeneous packing of 18:0/18:0 DGs, and 3% smaller than that found for the homogeneous packing of 18:0/18:2(n-6) DGs. However, the packing energies for the individual arrays differed. The array centered on 18:0/18:0 DG gave a value slightly larger than that for pure 18:0/18:0 DGs, whereas the array centered on 18:0/18:2(n-6) DG gave a much smaller value than that for pure 18:0/18:2(n-6) DGs. Such localized differences in packing energy may indicate that this particular mixture of DGs would show microheterogeneity on a scale of 10-20 Å, having small clusters of tightly packed molecules separated by more disordered regions.

Packing of 18:0/18:1(n-9) DG (Type 3 DGs)

We found maximal van der Waals contacts (see Methods) for a pair of 18:0/18:1(n-9) DGs when the second DG was rotated by 180° about the monolayer normal axis and placed so that the *sn*-2 faces were in contact in an antiparallel configuration. A hexagonal packing that incorporated this interaction had molecules in antiparallel rows, as in the Type 1 packing, but with each molecule rotated by about 30° around a normal to the monolayer (Table 1, **Fig. 6**). The rotation permitted antiparallel pairing of the monoenoic chains of two molecules from adjacent rows and allowed complementary filling of voids created by the kinked chains of each molecule. Although this packing could be considered to be an extremely distorted Type 1 packing, it seemed more useful to classify it as a distinct Type 3 packing unique to monoenoic DGs.

The packing permitted good contacts between saturated *sn*-1 chains in adjacent rows of molecules, but intermolecular contacts between *sn*-1 chains and *sn*-2 chains were impaired by the chain displacement at the double bonds. This displacement also reduced contacts between adjacent 18:1(n-9) chains that were not paired in back-to-back dimers. The various poor contacts created voids extending into the packed array from both the ester and hydrocarbon faces.

The cross-sectional area per molecule in the array was 10-12% larger than that of the areas obtained for the other DG models (Table 2), although lower than experimental values for monoenoic phospholipids (10). This packing showed a packing energy that was 30-40% smaller than the corresponding energies found for other model DGs in optimum Type 1 or Type 2 packings (Table 3).

DISCUSSION

The results of this investigation support the following conclusions. *1*) Each of the types of DG conformation identified in the companion report (2) is associated with a distinct type of packing arrangement. *2*) Proximally located angle-iron-shaped polyenoic sequences in the *sn*-2 chain of an *sn*-1-18:0 DG are associated with one type of regular packing, while distally located polyenoic sequences are associated with another. *3*) Favorable mixed packings are possible when DGs have the same type of regular conformation, but mixed packings of DGs of different conformation types are less favorable. *4*) All favorable packings have comparable packing energies,

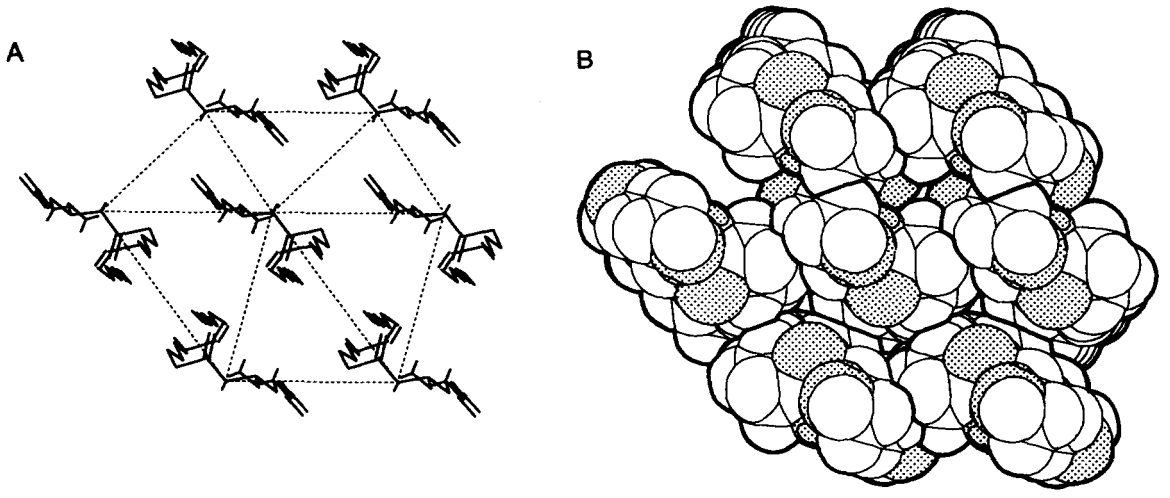

Fig. 6. Geometry of Type 3 18:0/18:1(n-9) DG packing cell. DG molecules are shown in Dreiding (A) and space-filling projections (B) as in Fig. 2.

packing densities, and cross-sectional areas. *5*) In contrast, DGs that contain an *sn*-2-18:1(n-9) group pack less favorably, and show smaller packing energies, lower packing densities, and larger cross-sectional areas.

One implication of our results is that polyenoic sequences in the *sn*-2-acyl chains of DGs and presumably also diacylglycerophospholipids may promote rather than prevent ordered packing arrangements in lipid bilayers. A further implication is that different types of polyenoic sequence may promote lipid clustering. However, whether these potential effects are actually realized in natural or artificial membranes remains to be determined. We modeled the packing of DGs rather than that of diacylglycerophospholipids because of the constraints of our modeling program. Moreover, we examined the DGs under a restricted set of conditions. The DGs all contained an *sn*-1-18:0 group, had conformations that resembled that of the diacylglyceryl moiety in crystalline 12:0/12:0 PE (7, 9), and were all oriented normal to the monolayer surface. In addition, we made no attempt to study effects of important variables such as temperature, hydrogen bonding, and degree of hydration, which critically influence the complex phase and packing behavior that exists in membranes (11-13).

Nevertheless, we believe that our results warrant careful attention because experimental support for our models exists. *1*) DGs incorporated into bilayers of liquid crystalline PC at a concentration of less than 10 mole percent appear to have conformations that are similar to those of our models (14, 15), though other conformations have been found for crystalline 12:0/12:0 DG (16) and 16:0/16:0 DG (17), and excess amounts of some DGs in phospholipid bilayers have been shown to induce the formation of hexagonal H_{II} phases (18, 19). *2*) Ernst, Sheldrick, and Fuhrhop (20) showed that crystals of the free acid forms of 18:2 (n-6), 18:3 (n-3), and 20:4 (n-6) contained extended acyl chains having a parallel orientation of double bonds. This led them to propose a polyenoic conformation that was similar to the angle-iron-shaped conformation in our models. *3*) Dratz and Deese (21) found that the C-D bonds of the olefinic carbons in bilayers of vinyl perdeuterated 16:0/22:6 (n-3) gave a unique, sharp NMR signal, characteristic of bonds oriented at the "magic angle" of 54.7° to the bilayer normal, and Baenziger and coworkers (22) reported similar results for the C-D bonds of the C28 methylene group in 16:0/18:2 (n-6) PC. These results imply that the double bonds in the liquid crystalline PCs were parallel to the bilayer normal, consistent with a helical or angle-iron-shaped conformation. *4*) Recent studies of monolayers of *sn*-1-16:0 PCs containing different *sn*-2 acyl chains at pressures of 30-40 mN/m revealed a large increase in area/molecule in going from a disaturated to an *sn*-2-monoenoic species, but showed smaller increases in going to dienoic and trienoic species, and showed no change or a decrease in going to species containing 4 or 6 double bonds (23, 24). These results imply that ordered chain packing was present, though the bulky choline head group (50-55 $Å^2$/molecule) may well have compromised such packing. *5*) A recent Raman spectroscopic study of PCs containing 1, 4, or 6 double bonds also provided evidence for ordered chain packing (25). *6*) Our Type 1 packing resembles the HS2 subcell found for a crystalline cerebroside (26), while our Type 2 packing resembles the HS1 subcell found for crystalline 12:0/12:0 PE (7), 16:0/16:0 PE (27), and the 17-bromoheptadecanoyl ester of cholesterol (28). For a review of subcell types and chain packing, see Abrahamsson et al. (29). The similarity between our Type 1 packing and the HS2 subcell becomes evident when the polyenoic angle-iron-shaped segments of the DG *sn*-2-chains are replaced by the planes through the methylene chain axes that bisect each angle-iron.

Further experimentation will be required to evaluate the importance of our modeling predictions. What is needed is a careful comparison of the physical properties of different well-characterized *sn*-1-18:0-polyenoic DGs and comparable phosphoglycerides. Very few studies of this type have been done to date. Investigators have tended to focus attention on the properties of commercially available lipids, such as disaturated lipids or dioleoyl lipids which do not adequately represent the polyenoic lipids that are typically found in animal cell membranes. NMR data and pressure/area isotherms for *sn*-1-18:0-polyenoic lipids with small head groups would be more likely to provide information of relevance to our models. In addition, studies of mixed packings of Type 1 and Type 2 polyenoic DGs, PEs, or PAs in liquid crystalline monolayers and bilayers might provide evidence concerning the potential effects of proximally and distally located polyenoic sequences on lipid clustering. The possibility that Type 1 and/or Type 2 lipids might cluster in natural membranes is of considerable potential interest because the clustering of these lipids might promote the formation of functionally important domains.

This investigation was supported by U.S. Public Health Service grant RR-00166 and by the Howard Hughes Medical Institute. We wish to thank the Regional Primate Research Center, University of Washington, for access to the Prophet workstation and to thank the San Diego Supercomputer Center for computing time allocated from a block grant of time assigned to the University of Washington.

Manuscript received 1 April 1991 and in revised form 9 July 1991.

REFERENCES

1. Applegate, K. R., and J. A. Glomset. 1986. Computer-based modeling of the conformation and packing properties of docosahexaenoic acid. *J. Lipid Res.* **27:** 658–680.
2. Applegate, K. R., and J. A. Glomset. 1991. Effect of acyl chain unsaturation on the conformation of model diacylglycerols: a computer modeling study. *J. Lipid Res.* **32:** 1635–1644.
3. BBN Systems and Technologies. 1990. The Prophet Primer. Release 3.1. BBN Systems and Technologies, Cambridge, MA.
4. BBN Systems and Technologies. 1990. Prophet Reference Manual. Release 3.1. BBN Systems and Technologies, Cambridge, MA.
5. BBN Systems and Technologies. 1990. CONTOUR. *In* Prophet Public Procedures. Release 3.1. BBN Systems and Technologies, Cambridge, MA. 25–27.
6. BBN Systems and Technologies. 1990. CAMCRYST. *In* Prophet Molecules. Release 3.1. BBN Systems and Technologies, Cambridge, MA. 240–272
7. Elder, M., P. Hitchcock, R. Mason, and G. G. Shipley. 1977. A refinement analysis of the crystallography of the phospholipid, 1,2-dilauroyl-DL-phosphatidylethanolamine, and some remarks on lipid-lipid and lipid-protein interactions. *Proc. R. Soc. Lond. A.* **354:** 157–170.
8. Hauser, H., I. Pascher, R. H. Pearson, and S. Sundell. 1981. Preferred conformation and molecular packing of phosphatidylethanolamine and phosphatidylcholine. *Biochim. Biophys. Acta.* **650:** 21–51.
9. Hitchcock, P. B., R. Mason, K. M. Thomas, and G. G. Shipley. 1974. Structural chemistry of 1,2-dilauroyl-DL-phosphatidylethanolamine: molecular conformation and intermolecular packing of phospholipids. *Proc. Natl. Acad. Sci. USA.* **71:** 3036–3040.
10. Smaby, J. M., A. Hermetter, P. C. Schmid, F. Paltauf, and H. L. Brockman. 1983. Packing of ether and ester phospholipids in monolayers. Evidence for hydrogen-bonded water at the *sn*-1 acyl group of phosphatidylethanolamines. *Biochemistry.* **22:** 5808–5813.
11. Phillips, M. C. 1972. The physical state of phospholipids and cholesterol in monolayers, bilayers, and membranes. *In* Progress in Surface and Membrane Science. J. F. Danielli, M. D. Rosenberg and D. A. Cadenhead, editors. Academic Press, New York. 139–221.
12. Pascher, I. 1976. Molecular arrangements in sphingolipids. Conformation and hydrogen bonding of ceramide and their implication on membrane stability and permeability. *Biochim. Biophys. Acta.* **455:** 433–451.
13. Gruner, S. M., P. R. Cullis, M. J. Hope and C. P. S. Tilcock. 1985. Lipid polymorphism: the molecular basis of monolayer phases. *Annu. Rev. Biophys. Biophys. Chem.* **14:** 211–238.
14. Hamilton, J. A., S. P. Bhamidipati, D. R. Kodali, and D. M. Small. 1991. The interfacial conformation and transbilayer movement of diacylglycerols in phospholipid bilayers. *J. Biol. Chem.* **266:** 1177–1186.
15. Hamilton, J. A., D. T. Fuhito, and C. A. Hammer. 1991. Solubilization and localization of weakly polar lipids in unsonicated egg phosphatidylcholine: a ^{13}C MAS NMR study. *Biochemistry.* **30:** 2894–2902.
16. Pascher, I., S. Sundell, and H. Hauser. 1981. Glycerol conformation and molecular packing of membrane lipids. The crystal structure of 2,3-dilauroyl-D-glycerol. *J. Mol. Biol.* **153:** 791–806.
17. Dorset, D. L., and W. A. Pangborn. 1988. Polymorphic forms of 1,2-dipalmitoyl-*sn*-glycerol: a combined X-ray and electron diffraction study. *Chem. Phys. Lipids.* **48:** 19–28.
18. Dawson, R. M. C., R. F. Irvine, J. Bray, and P. J. Quinn. 1984. Long-chain unsaturated diacylglycerols cause a perturbation in the structure of phospholipid bilayers rendering them susceptible to phospholipase attack. *Biochem. Biophys. Res. Commun.* **125:** 836–842.
19. Das, S., and R. P. Rand. 1986. Modification by diacylglycerol of the structure and interaction of various phospholipid bilayer membranes. *Biochemistry.* **25:** 2882–2889.
20. Ernst, J., W. S. Sheldrick, and J. H. Fuhrhop. 1979. The structures of the essential unsaturated fatty acids, crystal structure of linoleic acid, as well as evidence for the crystal structure of alpha-linolenic acid and arachidonic acid. *Z. Naturforsch.* **84b:** 701–711.
21. Dratz, E. A., and J. A. Deese. 1986. The role of docosahexaenoic acid in biological membranes: examples from photoreceptors and model membrane bilayers. *In* Health Effects of Polyunsaturated Fatty Acids in Seafoods. A. P. Simopoulos, R. R. Kifer and R. E. Martin, editors. Academic Press, New York. 319–351.
22. Baenziger, J. E., H. C. Jarrell, R. J. Hill, and I. C. P. Smith. 1991. Average structural and motional properties of a diunsaturated acyl chain in a lipid bilayer: effects of two *cis*-unsaturated double bonds. *Biochemistry.* **30:** 894–903.

23. Evans, R. W., and J. Tinoco. 1978. Monolayers of sterols and phosphatidylcholines containing a 20-carbon chain. *Chem. Phys. Lipids.* **22:** 207–220.
24. Evans, R. W., M. A. Williams, and J. Tinoco. 1987. Surface areas of 1-palmitoyl phosphatidylcholines and their interactions with cholesterol. *Biochem. J.* **245:** 455–462.
25. Litman, B. J., E. N. Lewis, and I. W. Levin. 1991. Packing characteristics of highly unsaturated bilayer lipids: raman spectroscopic studies of multilamellar phosphatidylcholine dispersions. *Biochemistry.* **30:** 313–319.
26. Pascher, I., and S. Sundell. 1977. Molecular arrangements in sphingolipids. The crystal structure of cerebroside. *Chem. Phys. Lipids.* **20:** 175–191.
27. Dorset, D. L. 1976. Aliphatic chain packing in three crystalline polymorphs of a saturated racemic phosphatidylethanolamine. *Biochim Biophys. Acta.* **424:** 396–403.
28. Abrahamsson, S., and B. Dahlen. 1977. The crystal structure of cholesteryl 17-bromoheptadecanoate. *Chem. Phys. Lipids.* **20:** 43–56.
29. Abrahamsson, S., B. Dahlen, H. Lofgren, and L. Pascher. 1978. Lateral packing of hydrocarbon chains. *Prog. Chem. Fats Other Lipids.* **16:** 125–143.